Mon. Not. R. Astron. Soc. **000**, 000–000 (0000) Printed 5 February 2008 (MN LaTeX style file v2.2)

arXiv:astro-ph/0606159v1 7 Jun 2006

Supermassive black hole formation during the assembly of pre-galactic discs

Giuseppe Lodato[1] and Priyamvada Natarajan[2,3]
[1] *Institute of Astronomy, Madingley Road, Cambridge, CB3 0HA*
[2] *Department of Astronomy, Yale University, P. O. Box 208101, New Haven, CT 06511-208101, USA*
[3] *Department of Physics, Yale University, P. O. Box 208120, New Haven, CT 06520-208120, USA*

5 February 2008

ABSTRACT

In this paper we discuss the evolution of gravitationally unstable pre-galactic discs that result from the collapse of haloes at high redshift $z \approx 10$ or so, which have not yet been enriched by metals. In cases where molecular hydrogen formation is suppressed the discs are maintained at a temperature of a few thousand degrees Kelvin. However, when molecular hydrogen is present cooling can proceed down to a few hundred degrees Kelvin. Analogous to the case of the larger scale proto-galactic discs, we assume that the evolution of these discs is mainly driven by angular momentum redistribution induced by the development of gravitational instabilities in the disc. We also properly take into account the possibility of disc fragmentation. We thus show that this simple model naturally predicts the formation of supermassive black holes in the nuclei of such discs and provides a robust determination of their mass distribution as a function of halo properties. We estimate that roughly 5% of discs resulting from the collapse of haloes with $M \approx 10^7 M_{\odot}$ should host a massive black hole with a mass $M_{\rm BH} \approx 10^5 M_{\odot}$. We confirm our arguments with time-dependent calculations of the evolution of the surface density and of the accretion rate in these primordial discs. The luminosity of the outer, colder disc is expected to be very low (in the range of a few thousand $L_{\odot}$), while the formation of the black hole is expected to produce a burst with a luminosity of a few times $10^9 L_{\odot}$. This mechanism offers an efficient way to form seed black holes at high redshift. The predicted masses for our black hole seeds enable the comfortable assembly of $10^9 M_{\odot}$ black holes powering the luminous quasars detected by the Sloan Digital Sky Survey at $z = 6$ for a concordance cosmology.

Key words: accretion, accretion discs – black hole physics – galaxies: formation – cosmology: theory – instabilities – hydrodynamics

1 INTRODUCTION

The local demography of black holes at the centers of galaxies suggests that black hole formation is a generic feature of galaxy formation (Magorrian et al. 1998; Tremaine et al. 2002; Ferrarese & Merritt 2000). Mergers and accretion processes, in fact, merger induced accretion are implicated in the assembly of black holes (Kauffmann & Haehnelt 2000; Volonteri et al. 2003; Di Matteo et al. 2005). However, all models require the formation of seed black holes at high redshift. The inferred large masses ($M_{\rm bh} \sim 10^9 M_{\odot}$) of the black holes powering luminous quasars at $z \sim 6$ detected by the Sloan Digital Sky Survey (SDSS) offers a challenge to mechanisms for production of seed black holes at higher redshifts (Fan et al. 2004). In a ΛCDM cosmology, these black holes have to assemble such large masses within a Gyr. The popular picture is that the remnants of the first generation of metal-free stars that form with an initial mass function that is biased towards higher masses (Abel et al. 2000; Bromm et al. 2002) provide the initial seed black holes with masses of the order of a 10's to 100 $M_{\odot}$ (Madau & Rees 2001; Volonteri et al. 2003; Ricotti & Ostriker 2004; Mapelli et al. 2006). Growing these seeds to the requisite masses by $z = 6$ to match the abundance of observed SDSS quasars requires various kinds of fine-tuning including phases of maximal growth powered by super-Eddington accretion. Volonteri & Rees (2005) consider the growth of black holes in metal-free halos with $T > 10^4$ K that cool via atomic hydrogen lines leading to the formation of a fat, gas disc. They argue that an episode of super-Eddington accretion assembles black holes with masses of $10^6\, M_{\odot}$ at $z \sim 15 - 20$.

There are alternative models that predict the direct formation of more massive seeds with masses of about

$10^5\,M_\odot$. These range from scenarios based on the formation of supermassive objects formed directly out of the collapse of dense gas (Haehnelt & Rees 1993; Umemura et al. 1993; Loeb & Rasio 1994; Eisenstein & Loeb 1995; Bromm & Loeb 2003; Koushiappas et al. 2004; Begelman et al. 2006). The key limiting factor for these models is the disposal of the angular momentum. One approach taken by Eisenstein & Loeb (1995) and Koushiappas et al. (2004) is to argue that it is preferentially either low spin halos with consequently low angular momentum gas or the low spin tail of the gas distribution in halos that can cool efficiently that form these seeds. Significant transfer of angular momentum is still required to go from the central massive object to the final collapsed hole that is expected to occur via the post-Newtonian instability. Non-axisymmetric structures like bars have been proposed (Shlosman et al. 1990) to efficiently transfer angular momentum at these late stages. In a recent paper, Begelman et al. (2006) have pursued this picture and argue that a low specific entropy 'quasi-star' is produced as a result of the cascade of the bars-within-bars instability leading to the formation of a black hole of a few solar masses.

In this paper, we argue for the formation of more massive black hole seeds ($\sim 10^5\,M_\odot$) from gas cooling in primordial halos via the growth of gravitational instabilities. We offer a picture wherein accretion processes and fragmentation criteria are addressed in a coupled fashion. The outline of our paper is as follows: in Section 2, we outline the scenario for pre-galactic disc formation in dark matter halos and discuss their accretion properties, the fragmentation criteria which determine the fate of the gas are discussed in Section 3 and the implied mass distribution of central concentrations is derived in Section 4. Detailed time-dependent models that confirm the analytic calculations in the previous sections are presented in Section 5, the resultant luminosity and potential observability of these sources is discussed in Section 6 followed by a discussion and implications of our work.

2 PRE-GALACTIC DISC FORMATION

In the context of the hierarchical, cold dark matter dominated structure formation paradigm, the baryonic components of galaxies assemble upon dissipation within dark matter halos. Generic to these models is the assembly of discs in these haloes as a consequence of dissipational collapse of the baryons (White & Rees 1978; Fall & Efstathiou 1980; Mo et al. 1998; Dalcanton et al. 1997). Here, we revisit some of the standard arguments put forward to describe the formation of proto-galactic discs inside a spherical dark matter halo of mass M. In particular, we adopt the formalism developed by Mo et al. (1998), and extend it to include the effect of angular momentum redistribution and mass accretion due to gravitational instabilities in the gas disc.

The arguments that form the basis of the standard disc formation picture are simple and elegant. It is assumed that a fraction $m_{\rm d}$ of the total mass of the halo, containing a fraction $j_{\rm d}$ of the angular momentum of the halo (usually assumed to be equal to $m_{\rm d}$), collapses and forms a disc. Note that the baryonic mass in the halo is assumed to be a fixed fraction of the halo mass, and the proportionality factor is taken to be the universal baryon fraction f_b. Assuming a radial profile for the resultant gas density distribution in the disc (for example, exponential) enables the calculation of its key physical properties: the disc scale length, central surface mass density, and crucially its stability under self-gravity. Star formation is then assumed to occur for those discs that are gravitationally unstable. The results of earlier work based on this paradigm depend on the detailed assumptions made. For example, while Mo et al. (1998) consider both an isothermal sphere and a NFW (Navarro et al. 1997) profile for the dark matter halo and a global criterion for gravitational instability, Oh & Haiman (2002) consider an NFW (Navarro et al. 1997) halo and a local instability criterion, based on the Toomre-Q parameter. These treatments present 'static' models for disc assembly. In this work, we examine the fate of these pre-galactic discs taking their time dependent evolution into account.

The limitation of previous analyses is that they consider the properties of the discs *a posteriori*, after all of their mass has been assembled, and do not consider the evolution of the discs *during* their formation process. They have argued that for some values of the relevant halo parameters, in particular, for low values of the spin parameter of the halo λ [1], the disc can be self-gravitating. In principle, these analyses also allow the disc to have very low values of Q or equivalently to be strongly unstable in terms of a stability criterion. However, it is important to note here that as soon as the disc becomes massive enough to be marginally stable, it will develop structures that will re-distribute angular momentum and mass through the disc, preventing the surface density from becoming too large and the disc from becoming too unstable. A suggestion that this kind of matter redistribution in primordial discs can lead to the formation of seed black holes was made recently by Begelman et al. (2006) and also, previously, by Koushiappas et al. (2004) but using substantially different arguments compared to our work here. In practice, the accretion of matter to the center will stop as soon as the surface density becomes low enough to make the disc stable, so that in the final state the disc will be exactly marginally stable. We explore this scenario and the consequences of angular momentum redistribution in detail here. In this section, we propose some simple arguments that allow us to estimate the final disc mass and the mass that will flow into the central region, leading to the formation and growth of a seed black hole. In Section 5 we support these simple arguments with full time-dependent calculations. We are therefore able to keep a detailed, self-consistent inventory of the fate of the gas.

We assume that in the final configuration, once the pre-galactic disc has assembled in the dark matter halo, only a fraction $m_{\rm f}$ of the total halo mass is retained in the disc (note that we track the baryons that remain in the disc and those that are accreted towards the center separately), while the remainder $m_{\rm a} = m_{\rm d} - m_{\rm f}$ is accreted towards the center of the galaxy providing fuel for a growing black hole. The final angular momentum per unit mass of the disc, however, remains equal to the initial value $j_{\rm d}$, since, in any accretion process, angular momentum is transported outwards, and the only loss of angular momentum due to accretion is related to the advection of it out of the inner radius of the disc. For an isothermal dark matter halo $\rho(r) \propto 1/r^2$ with a flat rotation curve, the angular momentum advected inwards due to the accretion of a mass $m_{\rm a}$ is $j_{\rm a} = j_{\rm d} R_{\rm in}/R_{\rm d} << j_{\rm d}$ (here $R_{\rm in}$ and $R_{\rm d}$ are the inner and outer radius of the disc, respectively). It is assumed here that the disc is embedded in a spherical, isothermal, dark matter halo, with virial temperature $T_{\rm vir}$ and a constant rotational velocity $V_{\rm h}$. To evaluate the stability of the disc, we use the Toomre parameter Q which is defined as:

---

[1] The spin parameter λ of a dark matter halo is defined as $\lambda = J\,|E|^{1/2}/G\,M^{5/2}$, where J is the angular momentum of the halo, E its total energy and M the halo mass.

$$Q = \frac{c_{\rm s}\kappa}{\pi G \Sigma} = \sqrt{2}\frac{c_{\rm s} V_{\rm h}}{\pi G \Sigma R}, \tag{1}$$

where $c_{\rm s}$ is the sound speed, $\kappa = \sqrt{2} V_{\rm h}/R$ is the epicyclic frequency, R is the cylindrical radial coordinate, and Σ is the surface mass density of the disc. We consider here the earliest generations of discs, which have not been metal-enriched and therefore are able to cool only through hydrogen. We present in the Appendix the detailed structure of these discs. Here we note that, in thermal equilibrium, if molecular hydrogen formation is *inhibited*, these discs are expected to be nearly isothermal at a temperature of a few thousand K. If molecular hydrogen is present, however, the disc can become much colder, with a temperature of a few hundred K. A marginally stable, isothermal disc has the same surface density profile as a Mestel disc (Mestel 1963). We therefore assume that:

$$\Sigma(R) = \Sigma_0 \left(\frac{R}{R_{\rm d}}\right)^{-1}. \tag{2}$$

Dark matter halos are characterised by their mass M and their angular momentum J, or equivalently by their spin parameter λ. The distribution of spin parameters for cold dark matter halos as determined from cosmological N-body simulations is given by:

$$p(\lambda){\rm d}\lambda = \frac{1}{\sqrt{2\pi}\sigma_\lambda} \exp\left[-\frac{\ln^2(\lambda/\bar{\lambda})}{2\sigma_\lambda}\right]\frac{{\rm d}\lambda}{\lambda}, \tag{3}$$

where the mean spin $\bar{\lambda} = 0.05$ and the dispersion is $\sigma_\lambda = 0.5$ (Warren et al. 1992). Requiring that the mass of the gas disc is a fraction $(m_{\rm d} - m_{\rm a})$ of the halo mass and that its angular momentum is a fraction $j_{\rm d}$ of the halo, following Mo et al. (1998) we easily get:

$$R_{\rm d} = 2\sqrt{2}\lambda \left(\frac{j_{\rm d}}{m_{\rm d}}\right) \frac{1}{1 - m_{\rm a}/m_{\rm d}} r_{200}, \tag{4}$$

$$\Sigma_0 = \frac{10}{16\pi}\frac{m_{\rm d}}{\lambda^2}\left(\frac{m_{\rm d}}{j_{\rm d}}\right)^2 \left(1 - \frac{m_{\rm a}}{m_{\rm d}}\right)^3 \frac{H(z) V_{\rm h}}{G}, \tag{5}$$

where $r_{200} = V_{\rm h}/10H(z)$ is the halo virial radius (the radius within which the density is 200 times the critical density of the Universe) and $H(z)$ is the Hubble constant as a function of redshift z. We can now evaluate Q, given the disc temperature $T_{\rm gas}$:

$$Q = \frac{8}{m_{\rm d}}\lambda \left(\frac{j_{\rm d}}{m_{\rm d}}\right)\left(\frac{T_{\rm gas}}{T_{\rm vir}}\right)^{1/2} \left(\frac{1}{1 - m_{\rm a}/m_{\rm d}}\right)^2. \tag{6}$$

We use the fact that the final disc configuration is exactly marginally stable, and thus obtain $m_{\rm a}$ by requiring that $Q = Q_{\rm c}$, a critical value above which the disc is gravitationally stable and no accretion can take place, due to the lack of an angular momentum transport mechanism. This gives:

$$\frac{m_{\rm a}}{m_{\rm d}} = 1 - \sqrt{\frac{8\lambda}{m_{\rm d} Q_{\rm c}}\left(\frac{j_{\rm d}}{m_{\rm d}}\right)\left(\frac{T_{\rm gas}}{T_{\rm vir}}\right)^{1/2}}. \tag{7}$$

Note that, although the result summarized in eqn. (7) is based on the assumption that angular momentum is redistributed within the disc, it does not depend on the specific viscosity mechanism, and is therefore very robust. The only assumption made is that whatever this mechanism is, it is only active when the disc is gravitationally unstable (a very reasonable assumption for such primordial discs, for which the main source of viscosity comes from gravitational instabilities). As shown, the amount of mass that will be concentrated in the central regions of these pre-galactic discs depends only on halo properties (such as the spin parameter λ and the fraction of baryonic mass that collapses to the disc $m_{\rm d}$), the ratio between gas temperature and halo virial temperature, and on the threshold value of Q, which has a very small range of variation around $Q_{\rm c} \approx 1$.

Equation (7) then provides a powerful link between the properties of dark matter haloes and the mass of massive, seed black holes that can grow within them. This implies a larger mass concentration in the center for haloes with low spin parameter λ or with high virial temperature $T_{\rm vir}$ (corresponding to higher halo mass mass M). The fact that seed black holes are likely to form preferentially in low spin halos was also demonstrated by Eisenstein & Loeb (1995) and by Koushiappas et al. (2004), using a different set of arguments. However, for high mass haloes, there is the added possibility that the disc fragments. We discuss the issue of fragmentation in Section 3 and we postpone to Section 4 the discussion of the mass distribution of central concentrations given the distribution of the spin parameter λ.

3 FRAGMENTATION CRITERIA

The arguments outlined in the previous section implicitly assume that, when the disc is gravitationally unstable, it is able to redistribute mass and angular momentum so as to accommodate the incoming mass inflow from the halo, maintaining a marginally stable state. Actually, in some cases, this is not going to be the case and the disc might undergo fragmentation. The criterion for the fragmentation of a gravitationally unstable disc has been studied extensively in the past few years (especially in relation to models of planet formation). Gammie (2001) has shown that being unstable (i.e. having $Q \lesssim 1$) is a necessary but not sufficient requirement for disc fragmentation. He has shown that fragmentation occurs only when the cooling time is faster than the disc dynamical timescale. An equivalent fragmentation criterion, that directly relates accretion and fragmentation properties, has been discussed by Rice et al. (2005). Indeed, they have shown that the gravitationally induced stress in a thin disc cannot exceed a critical value, which, measured in terms of the standard α description of transport properties of accretion disc, corresponds to $\alpha_{\rm c} \approx 0.06$. If the disc is required to provide a larger stress, by either strong cooling or by a large mass inflow, it will undergo fragmentation within a dynamical time-scale. In the context of pre-galactic discs that we are considering here, this will then lead to efficient star formation in the disc.

In the case considered here, the constraints imposed by cooling are not important, since, due to the steepness of the cooling function when the gas is predominantly hydrogen (in either the molecular or atomic form), slight changes in the temperature can easily bring the disc into thermal equilibrium. The constraint coming from the inflow of mass from the halo is much more important. The mass accretion rate $\dot{M}_{\rm h}$ from the halo can be simply estimated by requiring that a mass $m_{\rm d}M$ (where $M = V_{\rm h}^2 r_{200}/G$ is the total halo mass) collapses in a free-fall time-scale $t_{\rm ff} = r_{200}/V_{\rm h}$. We therefore get:

$$\dot{M}_{\rm h} = m_{\rm d}\frac{V_{\rm h}^3}{G}. \tag{8}$$

For a self-gravitating disc the standard mass conservation equation for a steady disc:

$$2\pi\nu\Sigma = \dot{M}, \tag{9}$$

where $\dot{M}$ is the mass accretion rate and ν is the viscosity (described here with the standard α-parameterization), takes the simple form:

$$\dot{M} = 2\alpha\frac{c_{\rm s}^3}{G}, \tag{10}$$

from which we see that in a steady state any isothermal disc will be characterized by a constant viscosity coefficient α. Note that in eqn. (9) there is a factor 2 rather than the standard factor 3 of Keplerian discs, because the rotation curve here is assumed to be flat.

What would happen to the transport properties in the disc once the fragmentation threshold is overcome is still not clear. A plausible assumption is that the accretion rate would be capped at its threshold value, with extra heating needed to reach thermal balance. This heat could be provided by the star formation process. The disc would then not be able to transfer down to its inner parts an $\dot{M}$ larger than:

$$\dot{M}_{\rm max} = 2\alpha_{\rm c}\frac{c_{\rm s}^3}{G}, \tag{11}$$

where $\alpha_{\rm c} \approx 0.06$.

If we consider the case of cooling via atomic hydrogen and assume that $T_{\rm gas} \approx 4000$ K, we find that $\dot{M}_{\rm max} \approx 10^{-2} M_{\odot}/{\rm yr}$. In contrast, for the cold discs arising when molecular cooling is efficient, the maximum accretion rate is significantly lowered, down to $\dot{M}_{\rm max} \approx 3\times 10^{-4} M_{\odot}/{\rm yr}$.

If the disc evolves to a steady state, one should expect that the mass flow in the disc would equal the inflow rate $\dot{M}_{\rm h}$. Actually, as the disc builds up, only a fraction of the matter flows into the inner disc, since the remaining has to be transported outwards to take up the angular momentum lost by in-flowing material. Since the viscous time-scale in the outer disc is very long, even if the inner disc is almost in a steady state, the inner flux $\dot{M}_{\rm in}$ will still be a fraction of $\dot{M}_{\rm h}$, that we will calculate explicitly in Section 5. We anticipate here the result that the mass flux in the inner disc is at most a fraction $f = 1/2(1 + m_{\rm a}/m_{\rm d})$ of the total inflow of matter. Note that $1/2 < f < 1$, so even in the extreme case where no mass in accreted (i.e. $m_{\rm a} = 0$), the mass flow is only reduced by a factor of a half. We expect fragmentation if:

$$\dot{M}_{\rm in} = m_{\rm d}\frac{V_{\rm h}^3}{G}\frac{1}{2}\left(1+\frac{m_{\rm a}}{m_{\rm d}}\right) > 2\alpha_{\rm c}\frac{c_{\rm s}^3}{G}. \tag{12}$$

We can rearrange eqn. (12) in terms of the ratio of the virial temperature to the gas temperature:

$$\frac{T_{\rm vir}}{T_{\rm gas}} > \left(\frac{4\alpha_{\rm c}}{m_{\rm d}}\frac{1}{1+m_{\rm a}/m_{\rm d}}\right)^{2/3}. \tag{13}$$

Assuming $\alpha_{\rm c} = 0.06$ and $m_{\rm d} = 0.05$, we can therefore identify three possible behaviours:

- $T_{\rm vir}/T_{\rm gas} \gtrsim 2.9$: these haloes will form discs that will fragment and form stars.
- $1.8 \lesssim T_{\rm vir}/T_{\rm gas} \lesssim 2.9$: these haloes will form fragmenting discs only if the spin parameter is significantly low, so that $m_{\rm a}/m_{\rm d} \sim O(1)$.
- $T_{\rm vir}/T_{\rm gas} \lesssim 1.8$: these haloes will not produce fragmenting discs, but since the halo mass is relatively low, the amount of mass that can be concentrated in the center will also be correspondingly low (cf. eqn. 7).

In practice, whenever it happens, fragmentation will act to suppress the concentration of the largest amount of mass in the center, whereas haloes with relatively smaller central concentrations are by and large unaffected by fragmentation.

The criterion for fragmentation described above, and the critical value of α, have been obtained in the context of thin and Keplerian discs. The haloes that give rise to large concentration of mass in the center have $T_{\rm vir} \gtrsim T_{\rm gas}$ and therefore the discs that form within them are relatively thick. In this case, the Jeans mass in a fragmenting disc is only slightly smaller than the total disc mass, so that fragmentation might be less likely in this case than for thin discs, effectively leading to an increase of the critical value of α.

4 MASS DISTRIBUTION OF CENTRAL CONCENTRATIONS

We now discuss the distribution of central mass concentrations, given a distribution of halo spin parameters. We determine the distribution of the mass available to feed a growing black hole in the center of the pre-galactic disc, $M_{\rm BH} = m_{\rm a}M$, based on eqn (7), while the distribution of λ is given by eqn. (3). We also need to specify the values of $m_{\rm d}$ and $Q_{\rm c}$. We assume $m_{\rm d} = 0.05$, but we also consider the case were $m_{\rm d} = 0.1$. As customary, we take $j_{\rm d} = m_{\rm d}$ (Mo et al. 1998). The critical value for the Q-parameter, $Q_{\rm c}$ is more uncertain. A self-gravitating disc is marginally stable to local, axi-symmetric instabilities at $Q = 1$. However, non axi-symmetric and global instabilities cause the disc to become unstable at larger values of Q. The prescription described above implies that at $Q = Q_{\rm c}$ the disc provides no stress, while on the other hand, Lodato & Rice (2004, 2005) have shown that a $Q = 1$ disc is able to deliver a sizable stress. We expect $Q_{\rm c}$ to be of the order of, but relatively larger than, unity and therefore consider two cases: (i) $Q_{\rm c} = 2$ and (ii) $Q_{\rm c} = 3$.

4.1 The case of atomic hydrogen cooling

First, we consider the case when molecular hydrogen formation is inhibited and the gas can consequently cool down

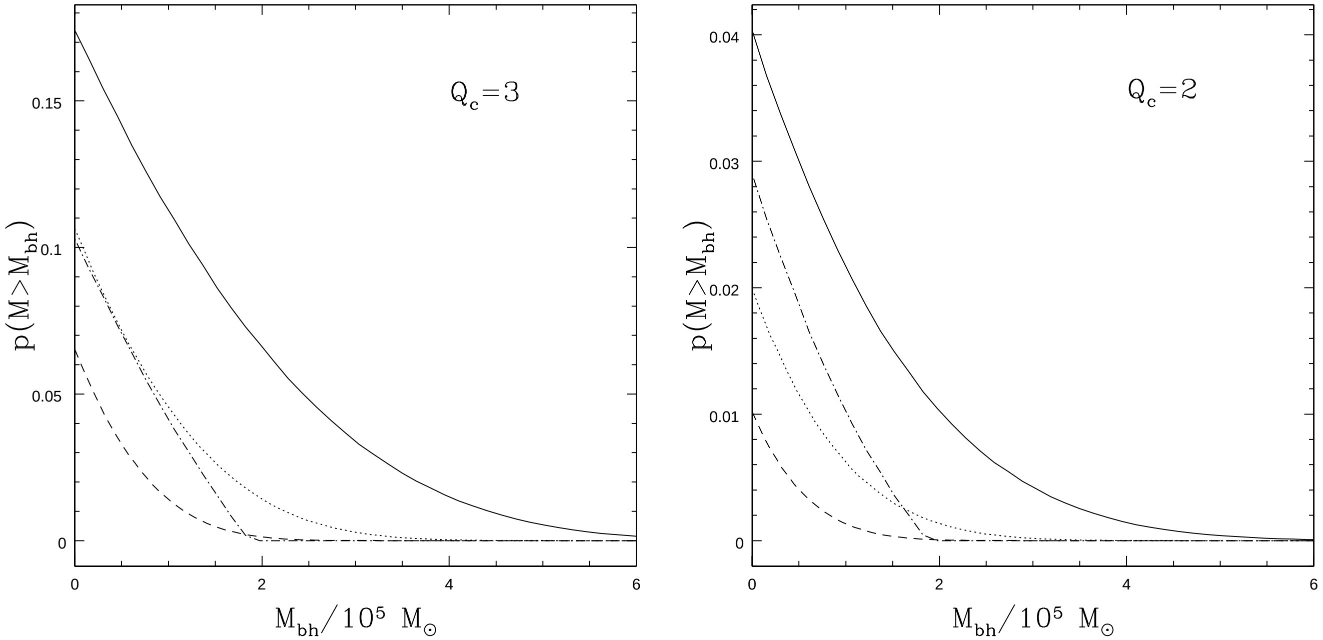

Figure 1. Cumulative distribution of the mass available to the formation of a seed black hole: The parent haloes are at a redshift $z = 10$ and we assume here that $m_{\rm d} = 0.05$. The line styles refer to $M = 3 \times 10^7 M_\odot$ (solid), $M = 2 \times 10^7 M_\odot$ (dotted), $M = 10^7 M_\odot$ (dashed). The dot-dashed line refers to the case of an $M = 3 \times 10^7 M_\odot$ halo, when fragmentation at the lowest λ is allowed. For the two lower halo masses fragmentation will not occur.

to $T_{\rm gas} \approx 4000$ K through atomic hydrogen cooling only (see Appendix for details). As discussed above, for a given $T_{\rm gas}$, haloes with larger $T_{\rm vir}$ produce larger central mass concentrations. However, we also have to require that the disc does not fragment, which then limits the analysis to $T_{\rm vir} \lesssim 3T_{\rm gas} \approx 10^4$ K. The typical redshift of collapse of haloes with this virial temperature is around $z \approx 10$.

In Fig. 1, we show the results for the two cases $Q_{\rm c} = 2$ and $Q_{\rm c} = 3$, respectively. For both cases, the haloes are assumed to be at a redshift $z = 10$ with mass in the range of $10^7 M_\odot$. The lines refer to 3 values of the halo mass, $M = 3 \times 10^7 M_\odot$ (solid line), $M = 2 \times 10^7 M_\odot$ (dotted line) and $M = 10^7 M_\odot$ (dashed line). While for the two lower mass cases $T_{\rm vir} \lesssim 1.8T_{\rm gas}$ and according to the results of the previous section, fragmentation is not expected to take place, for the highest mass case the disc might fragment for the lowest values of λ. The dot-dashed line refers to the case where the possibility of fragmentation is included and in this instance, we assume that these discs simply do not produce any central mass concentration.

It can be seen that, especially for the $Q_{\rm c} = 3$ case that a significant fraction of discs host central mass concentrations. For dark matter haloes of mass $M = 3 \times 10^7 M_\odot$, approximately 12% of discs have a central concentration of mass larger than $10^5 M_\odot$, while the same mass concentration can be achieved by only 6% of discs hosted in halos with $M = 2 \times 10^7 M_\odot$. The results obtained assuming $m_{\rm d} = 0.1$ for $M = 10^7 M_\odot$ (solid line) and $M = 0.7 \times 10^7 M_\odot$ (dotted line) are shown in Fig. 2. In both cases the possibility of fragmentation is included, but it only affects the lowest spin parameter halos, for which the probability is small to start with. The two panels refer again to two different choices of $Q_{\rm c}$. As expected, in this case, where a larger fraction of the halo mass collapses to the disc, the fraction of gravitationally unstable discs is larger, resulting in a larger probability of hosting a large mass concentration at the center.

4.2 The case of molecular hydrogen cooling

We now consider the case where molecular hydrogen can form and the disc therefore cools down to $T_{\rm gas} \approx 500$ K. In this case, discs forming out of haloes with $T_{\rm vir} \approx 10^4$ K will most likely fragment. However, an important point to note is that both the conditions for fragmentation, and the fraction of halo mass that will accumulate at the center only depend on the ratio $T_{\rm gas}/T_{\rm vir}$ as shown in eqn. (7). Therefore, the very same central mass accumulation $m_{\rm a}$ that can be obtained for a 4000 K disc can be obtained for a disc with a temperature ten times lower, provided that the halo virial temperature is reduced by the same amount (i.e., from $T_{\rm vir} \approx 10^4$ to $T_{\rm vir} \approx 10^3$). The typical redshift for the collapse of such haloes is $z \sim 20$, higher than the $z \sim 10$ assumed above. Since the halo mass scales as $M \propto T_{\rm vir}^{3/2}(1+z)^{-3/2}$, the same results shown in Figs. 1 and 2 would still hold for a $T_{\rm gas} \approx 500$ K disc, provided that the mass scale (of both the halo and of the central mass) is reduced by a factor ~ 100. The typical mass of a central concentration in this case is of the order of $10^3 M_\odot$. Our proposed mechanism might therefore also be relevant to the conditions just prior to the formation of the first stars.

5 TIME-DEPENDENT MODELS

In this section, we develop some time-dependent models to confirm the results obtained with the simple estimates in

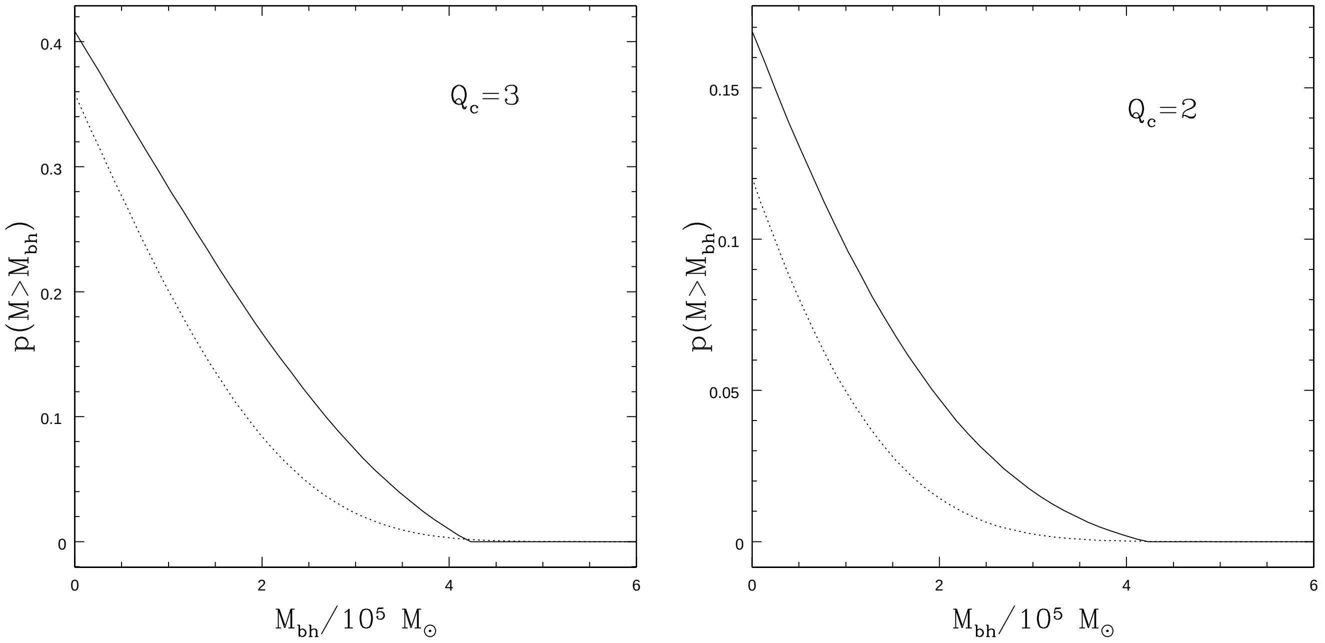

Figure 2. Cumulative distribution of the mass available for the formation of a seed black hole. The parent haloes are at a redshift $z = 10$ and we assume here that $m_{\rm d} = 0.1$. The line styles refer to haloes with mass $M = 10^7 M_{\odot}$ (solid) and $M = 0.6 \times 10^7 M_{\odot}$ (dotted).

previous sections. The evolution of the surface density Σ in a viscous disc with a flat rotation curve is given by:

$$\frac{\partial \Sigma}{\partial t} = \frac{1}{R}\frac{\partial^2}{\partial R^2}\left(\nu \Sigma R\right) + \dot{\Sigma}_{\rm in}, \tag{14}$$

where ν is the viscosity and $\dot{\Sigma}_{\rm in}$ is a source term representing the inflow from the halo.

It has been shown (Gammie 2001; Lodato & Rice 2004) that the transport associated with the development of such gravitational instabilities can be well described in terms of an effective viscosity, i.e. within the framework of the standard α description of accretion discs. It is then convenient to adopt the simple prescription for viscosity induced by gravitational instability described by Lin & Pringle (1990):

$$\nu = \alpha_{\rm g} c_{\rm s} H = \alpha_{\rm g}\frac{c_{\rm s}^3}{\pi G \Sigma}, \tag{15}$$

where $\alpha_{\rm g}$, the stress provided by gravitational instabilities, is modeled as:

$$\alpha_{\rm g} = \eta\left(\frac{Q_{\rm c}^2}{Q^2} - 1\right). \tag{16}$$

In the previous equation, $Q_{\rm c}$ is a critical value of Q, below which gravitational instabilities are able to provide a stress in the disc, and η is a parameter that essentially determines how far from the critical value of Q the disc has to be in order to deliver a given stress. In practice, the general behaviour of such discs is that they attain a given value of Q, such that the stress provided through $\alpha_{\rm g}$ is the value required to pass on the incoming flux $\dot{\Sigma}_{\rm in}$. Modifying the value of η merely changes the equilibrium value of Q at which this stress is provided. Effectively, apart from small changes to the normalization of Σ, the specific value of η does not affect our results, therefore confirming that the final state of the disc and the central accumulation of matter does not depend on the specific viscosity mechanism. We have generally chosen $\eta = 0.1$, but have also explored other values and do not notice any appreciable difference.

The mass input is modeled in such a way that the accretion rate from the baryons contained in the halo onto the disc $\dot{M}_{\rm h} = 2\pi \int \dot{\Sigma}_{\rm in} R {\rm d}R$ is given by eqn. (8) for $t < t_{\rm ff} = r_{200}/V_{\rm h}$ and vanishes for $t > t_{\rm ff}$. In this way, the total mass accreted onto the disc is a fraction $m_{\rm d}$ of the halo mass. The radial dependence of $\dot{\Sigma}_{\rm in}$ is determined under the constraint that the total accreted angular momentum is a fraction $j_{\rm d}$ of the halo angular momentum, with the assumption that $j_{\rm d} = m_{\rm d}$. This constraint, however, still leaves some freedom in the choice of $\dot{\Sigma}$. For example, the same result is obtained in the two extreme cases where all the mass is added to the disc as a δ-function centered at $R_0 = \sqrt{2}\lambda r_{200}$, or the case where $\dot{\Sigma}_{\rm in}$ has an exponential dependence on radius $\propto \exp(-R/R_0)$, with $R_0 = \lambda r_{200}/\sqrt{2}$.

The results of two of these time-dependent calculations arre shown in figs. 3 and 4 . Both of them refer to the following choice of parameters: $\lambda = 0.02$, $m_{\rm d} = 0.05$, $c_{\rm s}/V_{\rm h} = 0.7$, $Q_{\rm c} = 3$. Fig. 3 refers to the case where the matter is added as a δ-function, while Fig. 4 refers to the case where an exponential profile of $\dot{\Sigma}_{\rm in}$ is adopted. The left panels show the surface density in the disc at $t = 0.7,\ 0.8,\ 1 t_{\rm ff}$ and at the end of the simulation, when all the matter has collapsed to the disc and the disc becomes stable and is not accreting. The middle panels show the profiles of $\alpha_{\rm g}$ at $t = 0.7,\ 0.8,\ 1 t_{\rm ff}$. The right panels show the time evolution of the disc mass (solid line) and of the total mass accreted from the halo (dot-dashed line). The fraction of halo mass accreted in the center at the end of the simulation was $m_{\rm a} \approx 0.00688$ for the δ-function case and $m_{\rm a} \approx 0.0073$ for the exponential case, in very good agreement with the simple estimates obtained from eqn. (7).

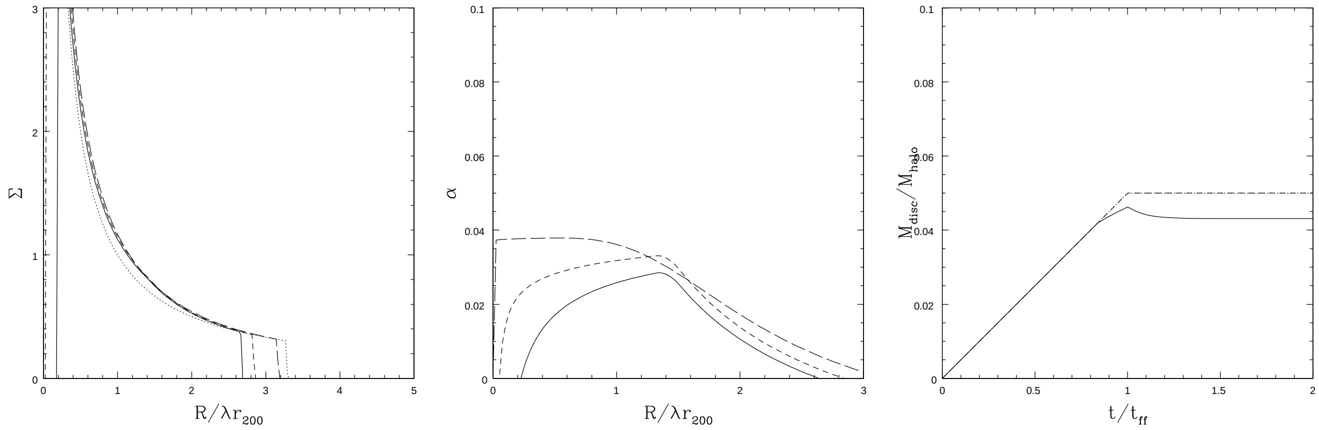

Figure 3. Results of a simulation where the mass is added to the disc with a δ-function, with $\lambda = 0.02$, $m_{\rm d} = 0.05$, $c_{\rm s}/V_{\rm h} = 0.7$ and $Q_{\rm c} = 3$. Left Panel: Surface density profiles (in units of $160 M_{\odot}/{\rm pc}^2$, assuming $T_{\rm gas} = 4000$ K and $z = 10$) at $t = 0.7, 0.8, 1 t_{\rm ff}$ (solid, short-dashed and long-dashed lines, respectively) and at the end of the simulation (dotted line). Middle Panel: Profiles of $\alpha_{\rm g}$ at $t = 0.7, 0.8, 1 t_{\rm ff}$ (solid, short-dashed and long-dashed lines, respectively). Right Panel: Time evolution of the disc mass (solid line) and of the mass collapsed onto the disc (dot-dashed line).

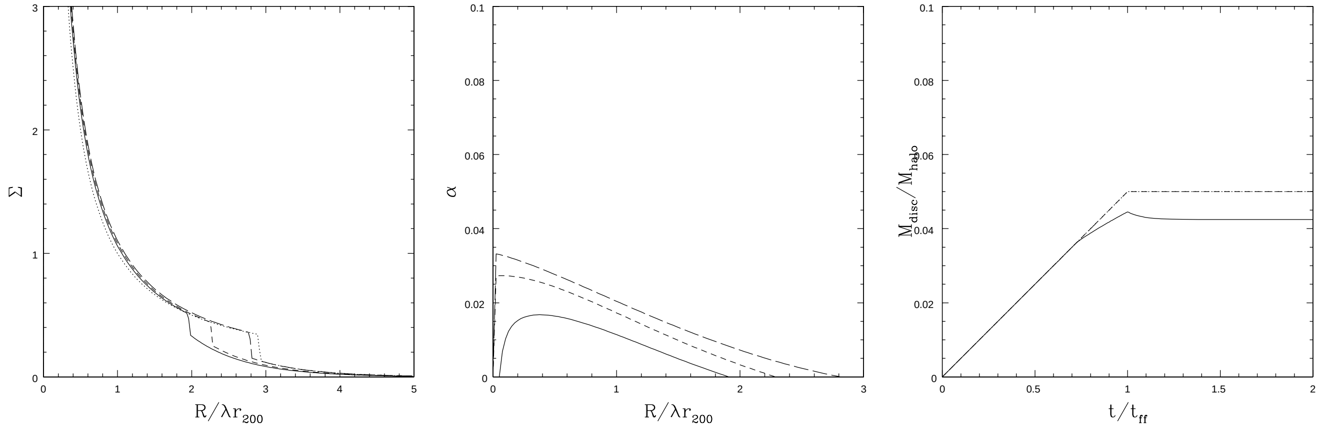

Figure 4. Results of a simulation where the mass is added to the disc with an exponential profile, with $\lambda = 0.02$, $m_{\rm d} = 0.05$, $c_{\rm s}/V_{\rm h} = 0.7$ and $Q_{\rm c} = 3$. Left Panel: Surface density profiles (in units of $160 M_{\odot}/{\rm pc}^2$, assuming $T_{\rm gas} = 4000$ K and $z = 10$) at $t = 0.7, 0.8, 1 t_{\rm ff}$ (solid, short-dashed and long-dashed lines, respectively) and at the end of the simulation (dotted line). Middle Panel: Profiles of $\alpha_{\rm g}$ at $t = 0.7, 0.8, 1 t_{\rm ff}$ (solid, short-dashed and long-dashed lines, respectively). Right Panel: Time evolution of the disc mass (solid line) and of the mass collapsed onto the disc (dot-dashed line).

A comparison of the evolution of disc mass for two cases with different values of $\lambda = 0.02$ (black line) and $\lambda = 0.01$ (dashed line) in shown in fig. 5. The other parameters were set as before and the mass input function was a δ-function. The accreted mass at the end of the simulation with $\lambda = 0.01$ is $m_{\rm a} = 0.019$, once again in very good agreement with eqn. (7).

An interesting feature that appears from these time-dependent models, is the value of the viscosity parameter $\alpha_{\rm g}$ during the simulation. If the disc were to deliver a steady mass accretion rate of $\dot{M}_{\rm h}$, as given by eqn. (8), it would require an $\alpha_{\rm g} = m_{\rm d}/2(V_{\rm h}/c_{\rm s})^3 \approx 0.07$ for the chosen parameters (comparing eqn. (8) with eqn. (10)). However, since the system is not in a steady state, the actual value of $\alpha_{\rm g}$ needed to provide the required mass flux is actually lower, peaking at roughly $\alpha_{\rm g} \approx 0.04$. This is quite important to determine whether we expect the disc to fragment and form stars or not. As described earlier, we expect fragmentation whenever the stress needed to transport the mass flux through the disc is larger than a threshold value $\alpha_{\rm c} \approx 0.06$. With the parameters chosen above, that requires $\alpha \approx 0.07$, we would then expect fragmentation, whereas in fact an evolving disc will always have a lower value effective of α and is therefore not expected to fragment.

The above behaviour can be understood quantitatively as follows: if some matter δM is delivered at a radius R_0, only a fraction $f = (1 - R_0/R_{\rm d})$ will flow into the inner disc, while the remaining $\delta M(R_0/R_{\rm d})$ will be carried out to compensate for the angular momentum lost by infalling matter. Of course, this will leave an unbalanced mass flux in the outer disc that will lead to an increase of $R_{\rm d}$. This however happens on a very long time-scale, especially since the viscosity in the outer disc becomes very small. Using

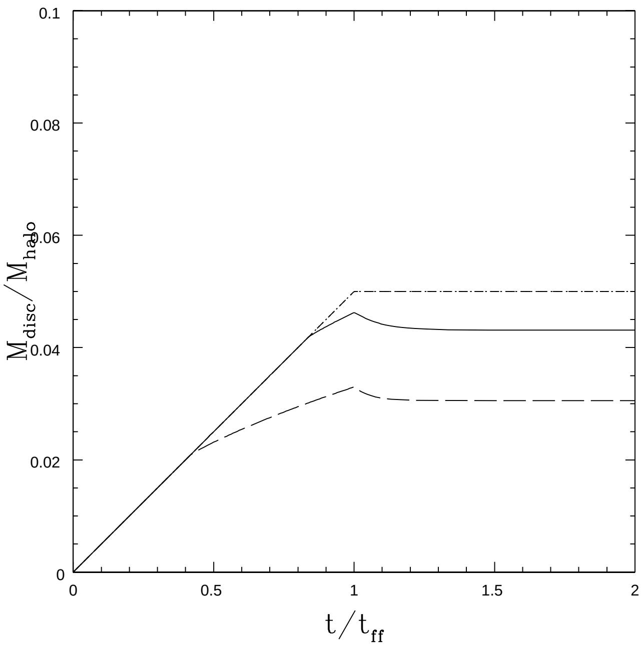

Figure 5. Comparison of the time evolution of the disc mass for two simulations with different values of the halo spin parameter: $\lambda = 0.02$ (solid line) and $\lambda = 0.01$ (dashed line). The dot-dashed line shows as in Figs. 3 and 4 the total mass collapsed onto the disc.

eqn. (4) to obtain the outer disc radius and assuming $R_0 = \sqrt{2}\lambda r_{200}$, we obtain:

$$f = \left(1 - \frac{\sqrt{2}\lambda r_{200}}{R_{\rm d}}\right) = \frac{1}{2}\left(1 + \frac{m_{\rm a}}{m_{\rm d}}\right), \qquad (17)$$

where we have also assumed $j_{\rm d} = m_{\rm d}$. For the case considered in Fig. 3, we obtain $f \approx 0.57$ which then lowers the required stress from $\alpha \approx 0.07$ to $\alpha \approx 0.04$, in perfect agreement with the results of the simulation. We have therefore demonstrated the result derived in Section 3 that the mass flow into the inner disc during the disc build up is actually smaller than its steady-state value by a factor f.

6 LUMINOSITY AND OBSERVABILITY

In this section we estimate the luminosity and potential observability these pre-galactic discs. Here we only concentrate on the hot discs dominated by atomic hydrogen cooling. The dissipation rate per unit surface area determined by the accretion process is:

$$D(R) = \nu\Sigma(R\Omega')^2 = \frac{\dot{M}}{2\pi}\left(\frac{V_{\rm h}}{R}\right)^2, \qquad (18)$$

where we have assumed a flat rotation curve at $V_{\rm h}$. The total luminosity emitted by the disc is:

$$\begin{aligned} L_{\rm disc} &= 2\pi\int_{R_{\rm in}}^{R_{\rm out}} RD(R){\rm d}R \\ &= \dot{M}V_{\rm h}^2\int_{R_{\rm in}}^{R_{\rm out}}\frac{{\rm d}R}{R} \approx m_{\rm d}\frac{V_{\rm h}^5}{G}\ln(R_{\rm out}/R_{\rm in}), \end{aligned} \qquad (19)$$

where $R_{\rm in}$ and $R_{\rm out}$ are the inner and outer disc radius, respectively, using $\dot{M} \approx m_{\rm d}V_{\rm h}^3/G$. The outer radius of the disc is given by $R_{\rm out} = R_{\rm d} \approx 100$ pc, for a gravitationally unstable disc, with $\lambda = 0.05$ at $z = 10$. The inner radius is harder to estimate. Our model will not be valid in the innermost parts of the disc, where the influence of a growing black hole will become important. Inside this radius the rotation curve will start to rise in an approximately Keplerian way, and the disc will therefore become hotter. This inner limiting radius can be estimated from:

$$R_{\rm in} = \frac{GM_{\rm BH}}{V_{\rm h}^2} \approx 4.5\times10^{-2}\left(\frac{M_{\rm BH}}{10^3M_\odot}\right)\left(\frac{10{\rm km/sec}}{V_{\rm h}}\right)^2 {\rm pc}. \qquad (20)$$

Substituting these values into eqn. (19), we find that the luminosity arising from the outer part of the disc is:

$$L_{\rm disc} \approx 4000L_\odot\left(\frac{V_{\rm h}}{10{\rm km/sec}}\right)^5. \qquad (21)$$

Note that, while in principle eqn. (21) would tell us that larger values of $V_{\rm h}$ would provide a much larger luminosity, this is actually unlikely, since for larger $V_{\rm h}$ the disc would efficiently fragment into stars rather than accrete at a higher rate, as discussed above. We therefore argue that the accretion luminosity in these discs is unlikely to exceed the estimate above. Since the gas cools mainly through atomic hydrogen line emission, most of this luminosity will be emitted in the Lyman series, and in particular in Lyα.

In fact, most of the luminosity of *the system* will be released in the inner disc, as the matter falls to the bottom of the potential well to ultimately form and feed the growing black hole. A detailed description of this process is beyond the scope of the present paper and has been discussed elsewhere (Volonteri & Rees 2005; Begelman et al. 2006). Indeed, the accretion rate onto the black hole or onto the 'quasi-star' described in such models is one of their input parameters. This parameter can be computed self-consistently in a time-dependent way based on our calculation presented in section 5. The results are shown in Fig. 3 and Fig. 6. The upper panel of Fig. 6 shows the time evolution of the mass of the growing central object $M_{\rm BH}$. The middle panel shows the evolution of the mass accretion rate onto it (solid line) and the corresponding Eddington rate for a black hole of mass $M_{\rm BH}$ with an efficiency of matter-luminosity conversion set equal to 0.1. As can be seen the initial phases are characterized by a strongly super-Eddington accretion phase (as expected, and as predicted by Volonteri & Rees 2005; Begelman et al. 2006). At later times, however, as the mass of the central object grows to reach roughly its asymptotic value, the accretion rate decreases, becoming sub-Eddington when the black hole has a mass of roughly $8\times10^4M_\odot$ in this case. The bottom plot shows the luminosity expected to be radiated from such a system, assuming that during the early super-Eddington phase the output luminosity is still limited by the Eddington value, while in the subsequent phase it is limited by the decrease in the mass supply. The peak of the luminosity is expected to occur just before the transition from the super- to the sub-Eddington regime and it corresponds to a few times $10^9L_\odot$.

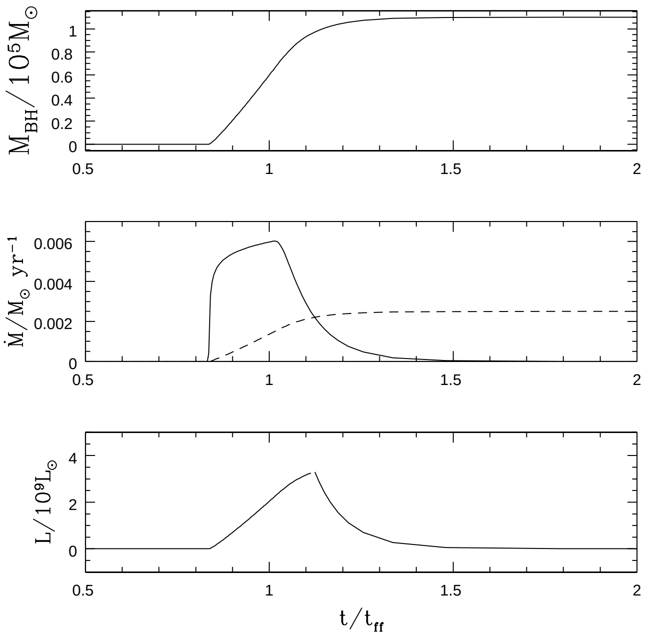

Figure 6. Upper Panel: mass of the central concentration as a function of time for the case shown in Fig. 3. Middle Panel: $\dot{M}$ in the inner disc (solid line) and the Eddington rate for a black hole of mass $M_{\rm BH}$ (dotted line). Bottom Panel: expected luminosity as a function of time, assuming that it is limited by the Eddington value at early times and by mass supply at late times.

6.1 Prospects for observing these pre-galactic discs

Given the low intrinsic luminosity of these pre-galactic discs ($\sim 4000\,L_\odot$), the prospects for direct detection are not promising. However, including the accretion luminosity of the black holes that are being assembled in the centers of these discs, they are likely to be detectable by the James Webb Space Telescope (JWST). The best strategy for detecting these objects is to exploit their lensing by foreground clusters. Using massive, foreground cluster-lenses as gravitational telescopes, we can expect to detect highly magnified pre-galactic discs. Therefore, a survey through cluster lenses by JWST is likely to be the most viable detection strategy.

7 DISCUSSION AND CONCLUSIONS

In this paper, we demonstrate that massive central concentrations can form naturally from pre-galactic discs that assemble in dark matter halos at high redshift. The masses of these concentrations depend on key properties of the host halo, mass, spin and gas cooling in the halo. In particular, low spin halos and massive halos are most efficient in concentrating gas in their centers. However, not all halos will be able to accrete gas into their centers. Taking into account the possibility of fragmentation furthers restricts the formation of eventual seed black holes. Using simple stability criteria, we predict that fragmentation and subsequent star formation are the fate for gas in some fraction of haloes. We derive 3 interesting regimes that are determined by the ratio of $T_{\rm vir}/T_{\rm gas}$, (i) if this ratio is greater than 2.9, haloes will form discs that will fragment and form stars and not directly form black holes; (ii) if this ratio lies between 1.8 - 2.9, haloes with low spin will lead to central mass concentrations; however, the lowest spin cases might be affected by fragmentation; (iii) if this ratio is lower than 1.8 the haloes will not produce fragmenting discs but will successfully accrete gas in their centers. Calculating the accretion rates for the fate of the accumulated gas we find super-Eddington rates leading to eventual black holes of masses up to $10^5 M_\odot$.

The model proposed here has two important predecessors in the work of Eisenstein & Loeb (1995) and in that of Koushiappas et al. (2004), but also presents significant differences with respect to both of them. Primordial gas acquires angular momentum through tidal interaction with the surrounding (Peebles 1969). This is generally measured through the parameter λ, the distribution of which can be determined from numerical simulations (Warren et al. 1992). Thus, the centrifugal barrier is the main obstacle to the formation of any compact object in the center of primordial galaxies. It is therefore not surprising that all models (including our own) predict that the most favourable sites for black hole formation are haloes with low spin. It is also not surprising that any black hole formation model has to deal with the problem of angular momentum removal. This issue was tackled in the work of Eisenstein & Loeb (1995), who calculated the viscous time-scale for primordial thin discs and assumed that black hole formation would only occur when the discs are so compact that their viscous time-scale is less than the typical time-scale for star formation. They found that only very rare haloes, with λ smaller by at least a factor 30 with respect to the average spin, would be able to produce black holes. This is substantially different from what we find here. Indeed, we find that even haloes with λ as large as 0.02-0.03 do produce large central mass concentrations. There are two main aspects with respect to which our model differs substantially from Eisenstein & Loeb (1995). The first one is the nature of the viscosity mechanism. Eisenstein & Loeb (1995) explicitly neglect the contribution of gravitational instabilities and assume that viscosity is driven by "turbulence". In standard accretion discs, turbulence is thought to arise from MHD instabilities (Balbus & Hawley 1998). However, for such primordial discs, where the primordial magnetic field is very weak and the gas is predominantly atomic or molecular, it is unlikely that MHD instabilities would be dynamically important. The second, and most important, difference is that Eisenstein & Loeb (1995) considered relatively thin discs, with $H/R \approx 0.03$, whereas our discs are substantially thicker. Since the viscous timescale is proportional to $(H/R)^{-2}$, this means that the viscous timescale as estimated by Eisenstein & Loeb (1995) is much larger than in our case. This in turn, is what leads to their more pessimistic estimate of the rarity of black hole forming haloes. Finally, a significant difference between our model and that of Eisenstein & Loeb (1995) is that our model naturally leads to a robust determination of the seed black hole mass function.

Koushiappas et al. (2004) propose that black hole seeds with masses of the order of $10^5 M_\odot$ (i.e. very similar to those obtained here) can form out of low angular momentum material in massive haloes. They assume that the lowest angular momentum material within the halo forms a compact disc which is gravitationally unstable and accretes onto the center due to the effect of an effective viscosity driven by the instability, in a way similar to what we propose here. However, they do not consider self-consistently the evolution of the surface density profile induced by the assumed viscosity mechanism. In their picture, the disc surface density simply grows linearly with time (at the same rate, independent of the radius) and at any given time it reflects the original angular momentum distribution of the gaseous component of the halo. On the contrary, what determines the surface density profile is actually the viscosity mechanism (which, being related to gravitational instabilities, in turn only depends on Q). As we have shown in Section 5 (Figs. 3 and 4), where we numerically follow the evolution of such discs, the final Σ profile (and the total accreted mass m_a) is the same whether we add mass to the disc with an exponential profile or with a δ-function, representing two extreme cases in the original angular momentum distribution within the halo. As a consequence of this, the estimates of black hole masses and their distribution given by Koushiappas et al. (2004) artificially depend on the initial angular momentum distribution and also on the assumed viscosity law. On the other hand, we have also clearly shown that, as long as viscosity is driven by gravitational instabilities, the black hole mass distribution is independent of viscosity.

In the present paper, for illustrative purposes, we have taken the simplifying assumption that these primordial discs live in the potential well of a simple isothermal sphere, with a given circular velocity V_h. For a more realistic density profile, the NFW profile (Navarro et al. 1997), in its innermost parts, the disc mass might dominate the potential well and become radially unstable, giving rise to bar-like instabilities. This, however, will leave our results and conclusions unaffected. Firstly, the instability criterion for such global instabilities (Christodoulou et al. 1995) is rather similar to our adopted criterion based on Q, and marginal stability is found to occur for equivalent values of $Q_\mathrm{c} \approx 2-3$, as adopted here. Secondly, since the disc mass is only a small fraction of the halo mass, only the innermost parts of the disc will be subject to bar-like instabilities, at radii much smaller than the typical disc radius R_d. The development of such instabilities might in fact enhance the accretion rate in the inner disc, but will not change the estimates of the total accreted mass obtained here. The important and interesting consequence of our model is that black hole masses of $10^9 M_\odot$ powering the luminous SDSS quasars at $z = 6$ can form comfortably within the available time of 1 Gyr in the concordance cosmology from our seed masses of $10^5 M_\odot$ at $z \sim 10$.

ACKNOWLEDGEMENTS

The authors acknowledge useful conversations and comments from Philip Armitage, Mitch Begelman, Cathie Clarke, Micheal Mayer, Jim Pringle and Marta Volonteri.

REFERENCES

Abel T., Bryan G. L., Norman M. L., 2000, ApJ, 540, 39

Balbus S. A., Hawley J. F., 1998, Reviews of Modern Physics, 70, 1

Begelman M. C., Volonteri M., Rees M. J., 2006, ArXiv Astrophysics e-prints

Bertin G., Lodato G., 1999, A&A, 350, 694

Bromm V., Coppi P. S., Larson R. B., 2002, ApJ, 564, 23

Bromm V., Loeb A., 2003, ApJ, 596, 34

Cen R., 1992, ApJS, 78, 341

Christodoulou D. M., Shlosman I., Tohline J. E., 1995, ApJ, 443, 563

Dalcanton J. J., Spergel D. N., Summers F. J., 1997, ApJ, 482, 659

Di Matteo T., Springel V., Hernquist L., 2005, Nature, 433, 604

Eisenstein D. J., Loeb A., 1995, ApJ, 443, 11

Fall S. M., Efstathiou G., 1980, MNRAS, 193, 189

Fan X., Hennawi J., Richards G., Strauss M., Schneider D., Donley J., Young J., Annis J., Lin H., Lampeitl H., Lupton R. H., Gunn J., Knapp G., Brandt W., Anderson S., Bahcall N., Brinkmann J., Brunner R., Fukugita M., Szalay A., Szokoly G., York D., 2004, AJ, 128, 515

Ferrarese L., Merritt D., 2000, ApJ, 539, 9

Galli D., Palla F., 1998, A&A, 335, 403

Gammie C. F., 2001, ApJ, 553, 174

Haehnelt M. G., Rees M. J., 1993, MNRAS, 263, 168

Katz N., Gunn J. E., 1991, ApJ, 377, 365

Kauffmann G., Haehnelt M., 2000, MNRAS, 311, 576

Koushiappas S. M., Bullock J. S., Dekel A., 2004, MNRAS, 354, 292

Lin D. N. C., Pringle J. E., 1990, ApJ, 358, 515

Lodato G., Rice W. K. M., 2004, MNRAS, 351, 630

Lodato G., Rice W. K. M., 2005, MNRAS, 358, 1489

Loeb A., Rasio F. A., 1994, ApJ, 432, 52

Madau P., Rees M. J., 2001, ApJ, 551, L27

Magorrian J., Tremaine S., Richstone D., Bender R., Bower G., Dressler A., Faber S. M., Gebhardt K., Green R., Grillmair C., Kormendy J., Lauer T., 1998, AJ, 115, 2285

Mapelli M., Ferrara A., Rea N., 2006, MNRAS, 368, 1340

Mayer M., Duschl W. J., 2005, MNRAS, 358, 614

Mestel L., 1963, MNRAS, 126, 553

Mo H. J., Mao S., White S. D. M., 1998, MNRAS, 295, 319

Navarro J. F., Frenk C. S., White S. D. M., 1997, ApJ, 490, 493

Oh S. P., Haiman Z., 2002, ApJ, 569, 558

Peebles P. J. E., 1969, ApJ, 155, 393

Pringle J. E., 1981, ARA&A, 19, 137

Rice W. K. M., Lodato G., Armitage P. J., 2005, MNRAS, 364, L56

Ricotti M., Ostriker J. P., 2004, MNRAS, 352, 547

Shlosman I., Begelman M. C., Frank J., 1990, Nature, 345, 679

Tremaine S., Gebhardt K., Bender R., Bower G., Dressler A., Faber S. M., Filippenko A. V., Green R., Grillmair C., Ho L. C., Kormendy J., Lauer T. R., Magorrian J., Pinkney J., Richstone D., 2002, ApJ, 574, 740

Umemura M., Loeb A., Turner E. L., 1993, ApJ, 419, 459

Volonteri M., Haardt F., Madau P., 2003, ApJ, 582, 559

Volonteri M., Rees M. J., 2005, ApJ, 633, 624

Warren M. S., Quinn P. J., Salmon J. K., Zurek W. H., 1992, ApJ, 399, 405

White S. D. M., Rees M. J., 1978, MNRAS, 183, 341

APPENDIX: THE STRUCTURE AND STABILITY OF SELF-GRAVITATING ZERO-METALLICITY ACCRETION DISCS

We consider the structure and stability of self-gravitating discs embedded in the external potential generated by a dark matter halo. If the disc is cold enough (or massive enough) it can become self-gravitating, i.e. it will develop gravitational instabilities. It is well known (Gammie 2001; Lodato & Rice

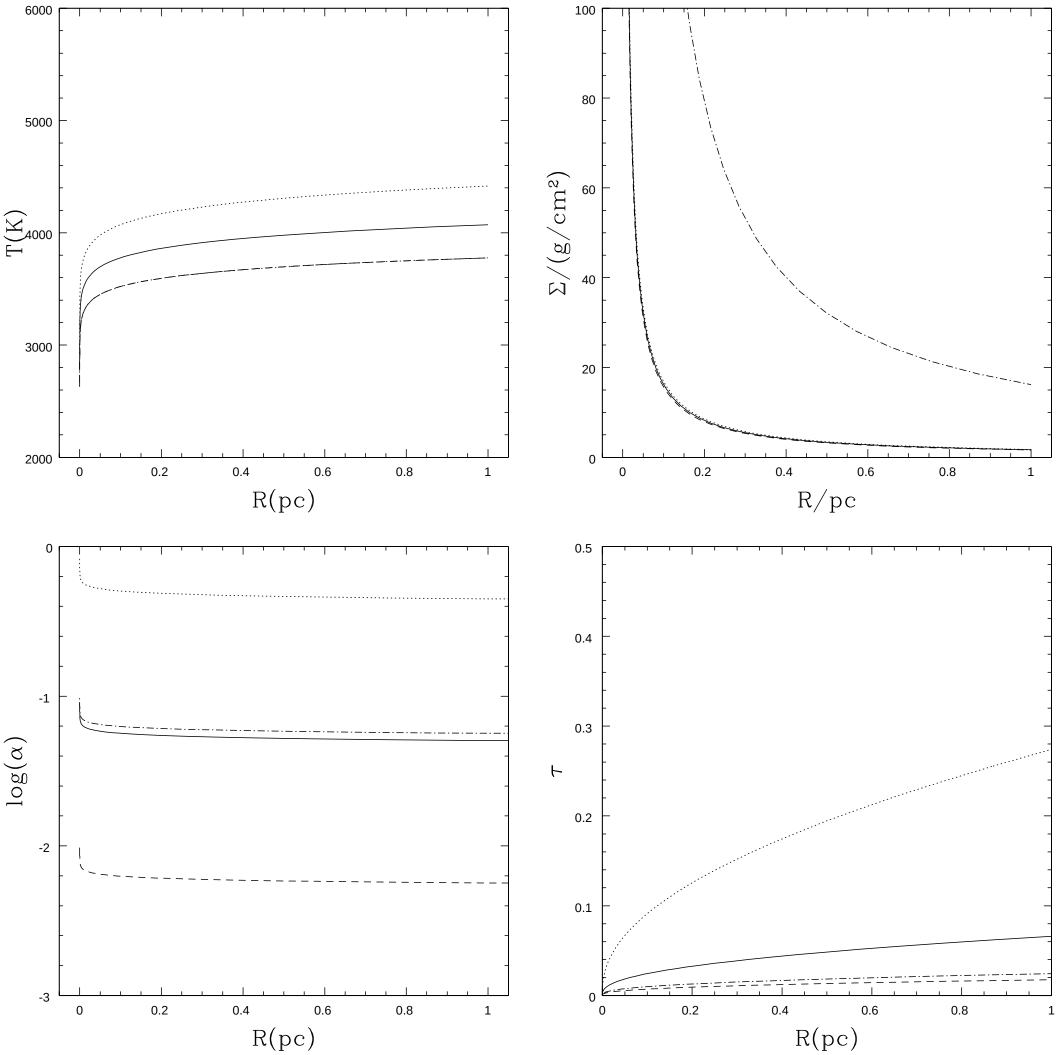

Figure 7. Structure of self-regulated accretion discs with cooling dominated by atomic hydrogen. The plots show (clockwise from top left): the temperature $T_{\rm gas}$, the surface density Σ, the optical depth τ and the viscosity coefficient α . The lines refer to the following pairs of $(\dot{M}, V_{\rm h})$: solid line $(10^{-2}, 10)$, dotted line $(10^{-1}, 10)$, dashed line $(10^{-3}, 10)$, dot-dashed line $(10^{-2}, 100)$, where $\dot{M}$ is in units of $M_{\odot}$/yr and $V_{\rm h}$ in km/sec.

2004, 2005) that once gravitational instabilities set in, the disc will rapidly evolve into a quasi-steady state of marginal gravitational instability, characterized by a constant profile of the Toomre parameter Q.

We start by noting that the requirement that Q be constant, for our flat rotation curve disc, implies that if the disc is isothermal (as it is expected to be, see Oh & Haiman 2002 and arguments below) then the surface density $\Sigma \propto R^{-1}$, i.e. the disc has the same density profile as a simple Mestel disc. This in principle, makes it very easy to include the contribution of the disc itself to the radial gravitational field, since it also leads self-consistently to a flat rotation curve. However, we will not consider this contribution at present. The steady state structure of such Mestel radially self-gravitating accretion discs has been explored extensively by Bertin & Lodato (1999), who also include the modifications to the disc structure expected to take place very close to the black hole, where its gravitational field starts to become important.

Actually, it is possible to solve for the detailed disc structure by relaxing the assumption of isothermality of the disc, and by computing the temperature by requiring that radiative cooling (here assumed to be optically thin) is balanced by the heating provided by the accretion mechanism. This energy balance equation gives us a relationship between α and the cooling time $t_{\rm cool}$ (Pringle 1981):

$$\alpha = \frac{1}{\gamma(\gamma-1)}\frac{t_{\rm dyn}}{t_{\rm cool}}, \tag{22}$$

where γ is the ratio of specific heats, $t_{\rm dyn} = R/V_{\rm h}$ is the dynamical timescale, and $t_{\rm cool} = nkT_{\rm gas}/n^2\Lambda(T_{\rm gas})$, where n is the number density, $T_{\rm gas}$ is the gas temperature and Λ is the relevant cooling function.

Once the cooling function is provided, it is then possible to solve the basic disc equations describing self-regulation (eqn. (1)), angular momentum conservation (eqn. (10)) and thermal equilibrium (eqn. (22)) for the three unknowns $\Sigma(R)$, $T_{\rm gas}(R)$ and $\alpha(R)$, with the input parameters Q, $\dot{M}$ and $V_{\rm h}$.

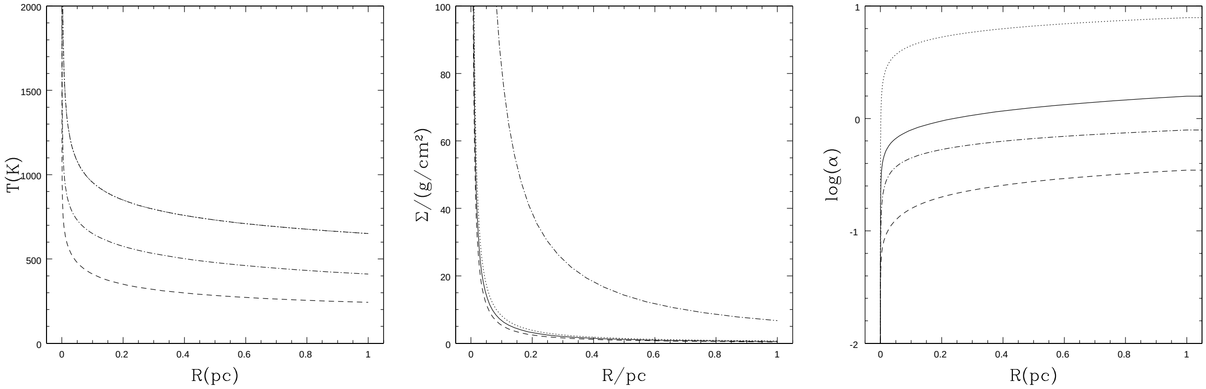

Figure 8. Structure of self-regulated accretion discs with cooling dominated by molecular hydrogen. The plots show (clockwise from top left): the temperature $T_{\rm gas}$, the surface density Σ, and the viscosity coefficient α. The lines refer to the following pairs of $(\dot{M}, V_{\rm h})$: solid line $(10^{-2}, 10)$, dotted line $(10^{-1}, 10)$, dashed line $(10^{-3}, 10)$, dot-dashed line $(10^{-2}, 100)$, where $\dot{M}$ is in units of $M_{\odot}$/yr and $V_{\rm h}$ in km/sec.

We consider here the case where the disc is made of primordial gas, with no metal enrichment. The cooling process is then going to be provided by hydrogen. We consider two cases: (a) when molecular hydrogen formation is suppressed, so that cooling is dominated by atomic hydrogen, and (b) the case where molecular hydrogen is present and therefore dominates the cooling function.

7.1 Cooling processes: Atomic hydrogen cooling

We consider here the cooling function for pure atomic hydrogen provided by Cen (1992) (we have also considered a different cooling function, after Katz & Gunn 1991, and found no significant difference). The results of the calculations are shown in Fig. 7 where we plot the resulting profiles of Σ, $T_{\rm gas}$ and α for different values of the input parameters. Here, we have assumed $Q = 1$ and varied $\dot{M}$ and $V_{\rm h}$. As can be seen, due to the steepness of the cooling function, the disc turns out to be almost isothermal, with the equilibrium temperature only very weakly dependent both on radius and especially on input parameters, with $T_{\rm gas} \approx 4000$ K (note that changing the mass accretion rate by two orders of magnitude, only modifies $T_{\rm gas}$ by roughly 14%). In Fig. 7, we also plot the optical depth of the disc $\tau = \Sigma\kappa_{\rm R}$, where the Rosseland mean opacities $\kappa_{\rm R}$ for a primordial composition has been taken from Mayer & Duschl (2005). We see that the assumption of optically thin cooling is indeed valid over the whole disc.

7.2 Cooling processes: Molecular hydrogen cooling

We consider next the situation wherein molecular hydrogen formation is not suppressed and we assume that it can form up to a molecular fraction $x_{H_2} = 10^{-3}$ (Oh & Haiman 2002). The cooling function for molecular hydrogen is taken from Galli & Palla (1998). Fig. 8 shows Σ, $T_{\rm gas}$ and α for this case. We do not plot the optical depth for molecular hydrogen cooling since the available opacity tables for primordial composition do not cover the very low temperature range predicted. At any rate, the opacity is expected to be extremely low. We can see that the equilibrium temperature is going to be much lower than in the case of atomic hydrogen cooling, as expected.

Since the cooling function is less strongly dependent on temperature for molecular hydrogen cooling, the "thermostat" that keeps the temperature of the disc constant in the case of atomic cooling is less efficient, and the equilibrium temperature in this case depends more strongly on the input parameters. The equilibrium temperatures range from 200 K to 700 K. The disc is still close to isothermal, with the temperature rising in the inner disc.